

図-5より、試験 No.①～③において、地表面の間隙水圧計の値(図中の記号●)が常に0kPaであることが分かる。このことから、これらの実験において地表面に水が溜まる現象は生じなかったといえる。また、CCDカメラの映像からも地表面に水が溜まる様子は確認されなかった。

各試験において、深さ20cm、15cm、10cmの間隙水圧計の値(図中の記号◆、□、■)が上昇開始する時間は、それぞれほぼ同時であった。このことより、散水された水が層を作って、一樣な速度で地盤内を浸透していったことが分かる。しかし、間隙水圧が上昇を開始してから値が落ち着くまでの時間は、それぞれの試験のケースで異なっている。試験 No.①と試験 No.②とを比較すると、表-1に示すように上層および下層共に試験 No.②の方が粘土分が多い。つまり、全体的に試験 No.②の方が粘土分が多いことにより、透水係数が下がったため、値が落ち着くまでの時間が長くなったと考えられる。また、試験 No.②と試験 No.③とを比較すると、上層において試験 No.③の方が粘土分が少ない。そのため、上層の透水係数が大きい分だけ試験 No.③の浸透速度が速くなったと考えられる。最後に試験 No.①と試験 No.③とを比較すると、下層において試験 No.①の方が粘土分が少ない。このため、試験 No.②と試験 No.③の比較で述べた様に、試験 No.①の方が浸透速度が速くなったと考えられる。これらの結果から、土中水は浸潤面を形成しながら浸透していき、その浸透速度は粘土分に依存していると判断できる。

3.2 間隙水圧の境界面における変化

図-5の各実験における0, 40, 80, 120, 600secにおける各深さの間隙水圧計の値を用いて、降雨開始からの間隙水圧分布の変化を図-6, 7, 8に示す。上層、下層ともに試料は飽和度50%になるように模型地盤を作製したため、降雨を開始する前の地下水面は深さ10cm付近に生じて、地下水面より上側の不飽和地盤の場所において-2~-7kPaの微小なサクションが計測された。しかし、降雨を開始して時間が経つにつれ、地下水面が上昇していき、このサクションは喪失した。また、降雨を終了した後、模型地盤全体が静水圧に近い三角形分布になっていることが分かる。

上層と下層の境界面(深さ5cm)の間隙水圧の変化に着目してみる。図-6に示す試験 No.①において、境界面の間隙水圧分布には大きな変化は見られなかった。これは、上層(粘土分0%)と下層(粘土分5%)は共に降雨強度(30mm/hr/G)に比べ透水係数が大きく、降雨によってもたらされた水分は地中に溜まらず、浸透していったためだと考えられる。図-7, 8に示す試験 No.②と③における0sec(図中の記号●)と40sec(図中の記号▲)を比較すると、境界面の間隙水圧だけが增加しているのが分かる。これは、下層(粘土分10%)が、試験 No.①と比べ粘土分が増加したことにより透水係数が小さくなったため、水分は全て下層に浸透せず層の境界面に溜まったと考えられる。また、試験 No.②と試験 No.③の上層は、粘土分5%と10%なので透水係数に差があるにも関わらず、境界面の間隙水圧の変化に明確な差が見られなかった。これは、粘土分0%、5%の場合には降雨強度に比べ透水係数が充分大きいため、浸透の状況に明確な差が出なかったと考えられる。つまり、今回の二層平面地盤の降雨実験より、30mm/hr/Gの降雨強度では、粘土分0%と5%に対する透水係数が大きいため、水は下層に完全に浸透する。しかし、粘土分10%は透水係数が小さくなるため、水は完全に浸透せずに境界面に溜まることが確認できた。

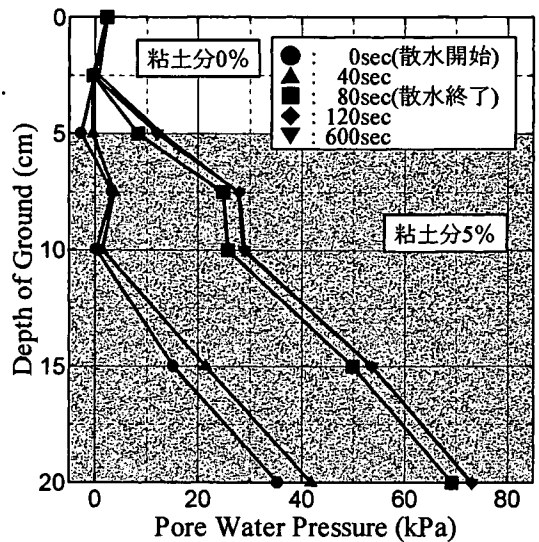


図-6 間隙水圧分布 (試験 No.①)

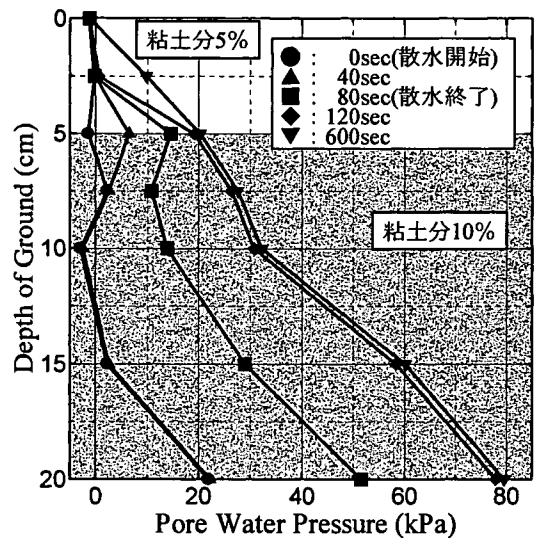


図-7 間隙水圧分布 (試験 No.②)

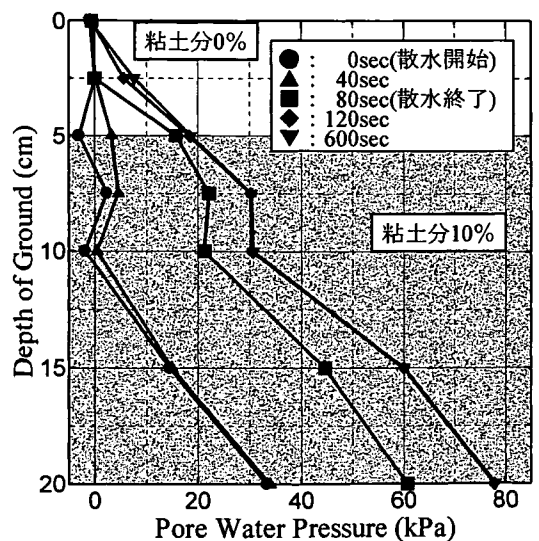


図-8 間隙水圧分布 (試験 No.③)

4.二層斜面地盤

4.1 間隙水圧の時間的变化

表-2 に二層斜面の降雨実験における実験条件を示す。また、図-9 には降雨開始後からの設置された間隙水圧計（図-2 参照）で計測された間隙水圧の時間变化を示す。また、試験 No.⑥ と試験 No.⑦ においては上層の部分で共に降雨中に斜面崩壊が確認された（図-10 参照）。図-10 は試験 No.⑦ の写真である。

表-2 二層斜面地盤降雨実験条件

試験No.	遠心加速度(G)	上層	下層	降雨強度(mm/hr/G)	降雨量(L)	降雨時間(sec)
④	40	粘土分0%	粘土分5%	30	1.0	33
⑤	40	粘土分5%	粘土分10%	30	1.0	33
⑥	40	粘土分0%	粘土分10%	30	1.0 <td 33	
⑦	40	粘土分0%	粘土分10%	15	1.0	66

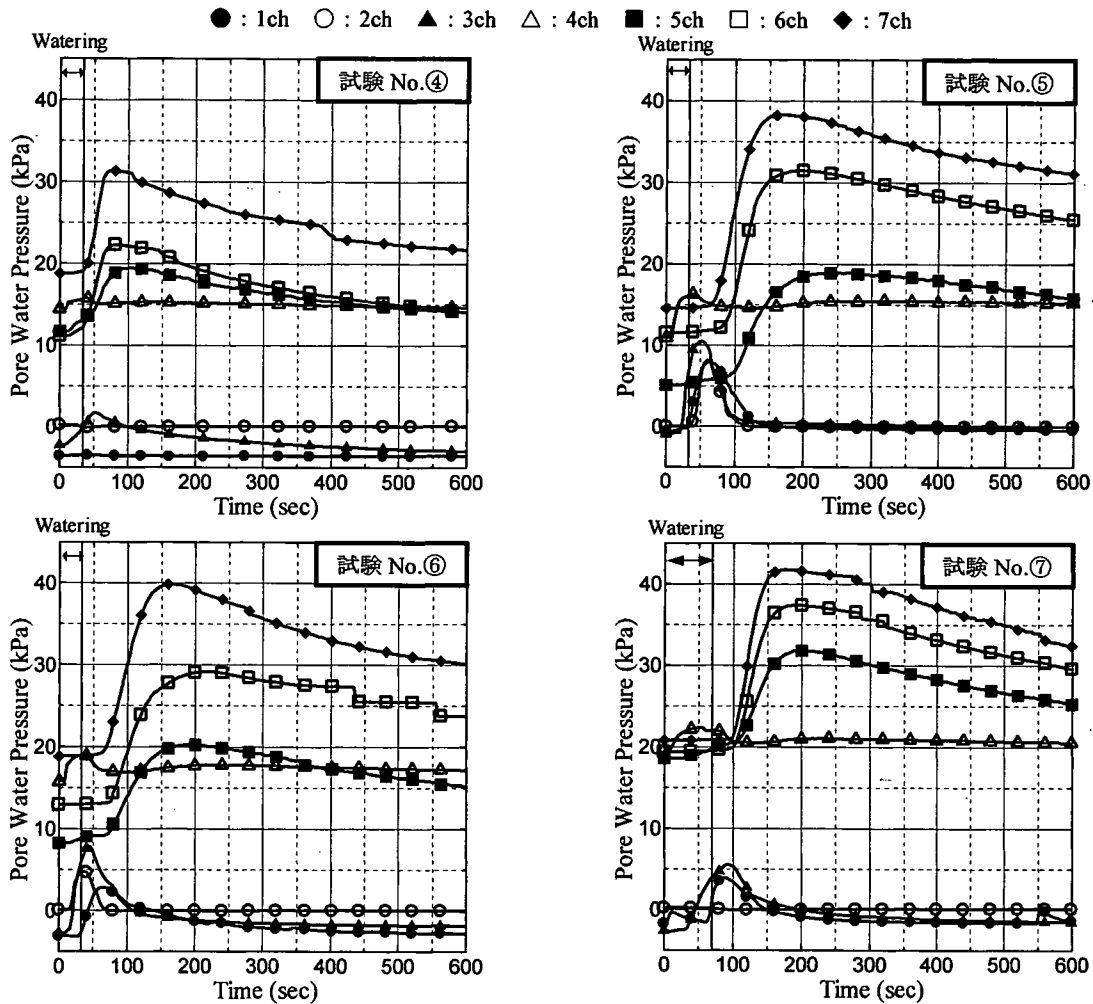


図-9 二層斜面降雨実験の間隙水圧変化

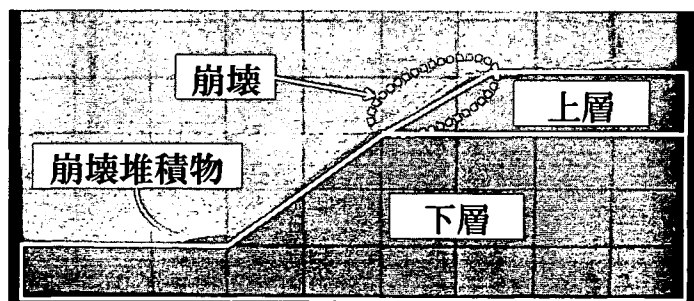
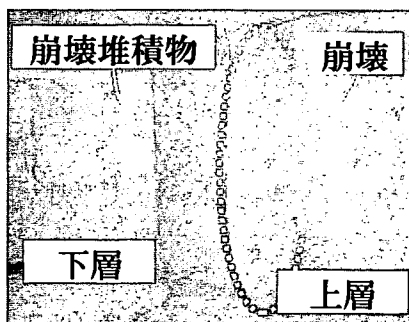


図-10 斜面崩壊の様子（左写真：上から、右写真：側面から）

図-9に示す4ch(図中の記号△, 設置位置は排水口下, 図-2参照)の間隙水圧の変化を見ると, 値はほぼ一定値を示しているのが分かる. これは二層斜面の降雨実験では排水口を設けて実験を行ったため, 法先部に水が溜まらず, 正常に排水が行われていたことを示す. また, CCDカメラからも法先部に水が溜まる現象は確認されなかった.

各試験条件において間隙水圧の値の変化について着目すると, 実験条件によって間隙水圧の値のピークが異なっている. 値が一番大きな7ch(図中の記号◆)に注目すると, 試験No.④が他の結果に比べピークの値が小さいことがわかる. 試験No.④は, 表-2に示すように, 他の実験結果に比べ上層および下層の粘土分が小さい. このため, 透水係数が他の実験に比べ大きく, 二層平面の降雨実験で述べたように降雨強度(速度)より浸透速度が, 地下水面が上昇する速度より早くなり, 地盤内の水分が排水口より排水されるためと考えられる. 試験No.⑤と⑥の7chのピーク時の間隙水圧を比較すると, わずかであるが試験No.⑥の方が値が大きくなっていることが分かる. これは, 上層の粘土分が5%から0%へと減少したことにより, 降雨が浸透する量(斜面表面を流れない量)がわずかに増加したためだと考えられる. また, 試験No.⑥と⑦とを比較すると, 同じ地盤条件であるが試験No.⑦の方が値が少し大きくなっていることが分かる. これは降雨強度が減少したために地盤に浸透する量が増えるので, 斜面表面を流れる量が相対的に減少したと考えられる. 以上の実験結果をまとめると, 間隙水圧のピークの値は, 以下の二つの要因から支配されていると考えられる. A) 粘土分が少ない(透水係数が大きい)と, 土中水は地盤内に溜まらず排水され, 間隙水圧のピークの値は減少する. B) 降雨強度を増加させると, 斜面表面を流れる水の量は増え, 間隙水圧のピークの値は減少する. しかし, B)による変化はA)による変化に比べ微小である.

次に間隙水圧の値がピークを示す時間について検討する. これは上層, 下層で粘土分が異なるので, 層ごとに着目して述べる. まず, 下層(5・6・7ch, 図中の記号■・□・◆)の間隙水圧は, 試験No.④だけが降雨開始70sec付近でピークとなり, 試験No.⑤, ⑥, ⑦では150sec付近でピークとなっているのが分かる. これは, 下層の粘土分の影響によるものと考えられる. つまり, 粘土分が増加したことにより, 水分の浸透する時間に変化が生じたためと考えられる. また, 上層(1・2・3ch, 図中の記号●・○・▲)に注目すると, 試験No.⑤, ⑥では降雨開始50sec付近で間隙水圧はピークとなり, 試験No.⑦では100sec付近でピークとなっている. これは, 下層の透水係数の大小によるものではなく, 降雨強度(降雨強度の減少により, 浸透速度も低下した)もしくは降雨時間(降雨時間が増えたことにより, ピークを刻む時間も遅れた)によるものだと考えられる. 今回の実験結果からでは, どちらの影響を受けたかは明確に述べられないので, 今後, 様々な実験条件で実験を行い検討していく必要がある.

4.2 地下水面変化

図-11に, 図-9における各時間の間隙水圧の値を用いて地下水面の変化を示した(間隙水圧は静水圧と仮定).

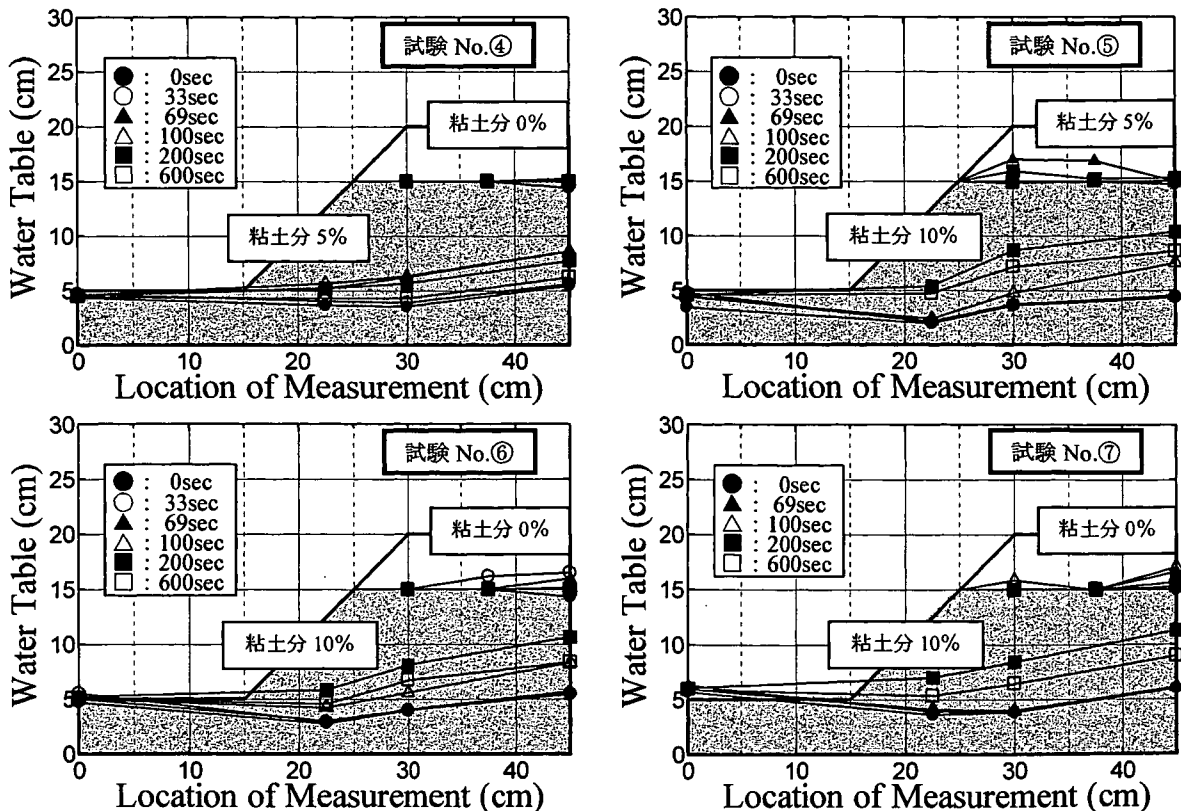


図-11 地下水面変化

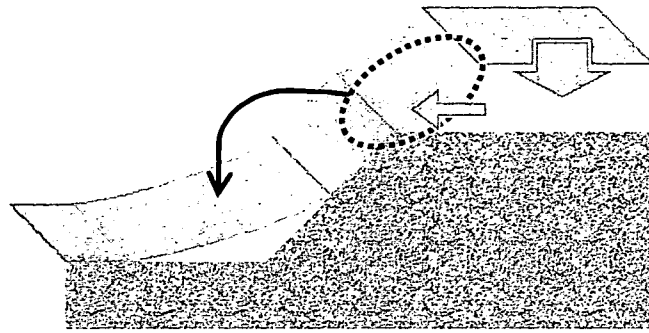


図-12 斜面崩壊メカニズム

図-11 から、全ての実験結果において、初期地下水面（0sec、図中の記号●）は、ほぼ排水口と同じ高さとなっていることが分かる。そして、降雨後の地下水面は時間が経つにつれ、初期地下水面に戻っていくことが確認された。また、試験 No.④の地下水面の変化を見ると、降雨によっても地下水面はほぼ変化していないことが分かる。これは、二層平面地盤の降雨実験の試験 No.①から得られた結果と同様、地盤の粘土分が少ないため透水係数が大きく、浸透量より排水量の方が大きくなったためだと考えられる。そして、他の二層平面地盤の降雨実験結果から推測すると、試験 No.⑤、⑥、⑦では試料の境界面に土中水が溜まり、地下水面が形成されるはずであるが、試験 No.⑥、⑦では明確な地下水面は観測されず斜面の崩壊が生じた。これは、上層の透水係数の違いによる影響と考えられる。試験 No.⑤、⑥、⑦では上層と下層の境界面に土中水が溜まろうとしたが、試験 No.⑥、⑦の上層は試験 No.⑤より粘土分が少ないため、境界面に溜まろうとした土中水は下層に浸透するより早く斜面表面より流れ出したと考えられる。この時に、斜面表面から排出される土中水によって崩壊が生じたと考えられる（図-12 参照）。試験 No.⑥、⑦の斜面が崩壊したことより、斜面崩壊の主要因は、降雨強度より斜面を構成している土の特性（粘土分や透水係数等）に依存していると今回の結果から言える。しかし、今回の実験条件は限られているので、今後さらに実験条件を増やす必要がある。

5. 結論

5.1 二層平面降雨実験

- ① 土中水は浸潤面を形成しながら浸透していき、その浸透速度は粘土分に依存している。
- ② 降雨強度 30mm/hr/G に対して、粘土分 0%、5%は水が地表面に溜まることなく浸透した。また、二層地盤では粘土分 10%の層の上部に地下水面が形成された。

5.2 二層斜面降雨実験

- ① 間隙水圧のピークの値は、以下の二つの要因から変化すると考えられる。
 - A) 粘土分が少ないと、土中水は地盤内に溜まらず排水され、間隙水圧のピークの値は減少する。
 - B) 降雨強度を増加させると、斜面表面を流れる水の量は増え、間隙水圧のピークの値は減少する。しかし、B) による変化は A) による変化に比べ微少である。
- ② 間隙水圧の値は、降雨後しばらく経ってからピークを向かえる。下層側の間隙水圧がピークとなるタイミングは、粘土分による影響がある。上層側の場合は、降雨強度や降雨時間の影響があると考えられる。
- ③ 粘土分が異なる斜面において、粘土分（透水係数）の差が大きくなると、土中水は浸透せず、斜面表面から排水されていく。その際に、斜面崩壊が生じる。

【謝辞】

本研究は、厚生労働科学研究費（労働安全衛生総合研究事業）「斜面崩壊による労働災害防止に関する研究」の補助を受けて実施されました。記して謝意を表します。

《参考文献》

- 1) 金子広明, 笠間太樹, 田中洋行, 工藤豊: 遠心模型実験装置を用いた降雨再現実験での間隙水圧の挙動, 第 42 回地盤工学会研究発表会, pp.533-534, 2007.
- 2) 笠間太樹, 金子広明, 田中洋行, 工藤豊: 遠心場における降雨実験での間隙水圧の挙動, 地盤工学会北海道支部年次技術報告集, 第 47 号, pp.167-170, 2007.

FAILURE MECHANISM OF SLOPES IN THE CENTRIFUGE USING IN-FLIGHT EXCAVATOR

S.B. Tamrakar¹⁾, Y. Toyosawa²⁾, K. Itoh³⁾, N. Horii⁴⁾ and S. Kusakabe⁵⁾

ABSTRACT

In this paper, failure mechanism of slopes during the excavation of lower portion of the slope (toe) is described. Model slopes of volcanic soils were prepared within the centrifuge and the slope was excavated using an in-flight excavator which could work within the centrifugal environment. Three types of statically compacted model slopes (100, 150 and 200 kPa) and two types of excavation pattern (toe excavation with or without trench excavation at the beginning) were studied. Direct contact type linear variable differential transducers (LVDT) were installed on the slope and on the top surface (crest) of the models to observe the deformation behaviour during the excavation. Circular slope failure was observed in all the cases. It was observed that the critical height of the slope before failure increases with the increase in the compaction pressure. In addition, if the excavation of toe of the slope is done with trench excavation at first, the critical height of the slope could be reduced in comparison to the excavation of toe without trench at first. From the deformation-elapsed time graph, 2nd and 3rd degree creep could be distinguished which might be helpful in the predicting the slope failure time.

KEYWORDS: toe excavation, centrifuge, in-flight excavator.

INTRODUCTION

Slope failure of the natural slopes occurs either due to natural phenomenon (rain, earthquake, etc.) or due to the manual construction works (excavation, embankment, etc.). To protect the slopes, either they are excavated up to the stable (safe) slopes or gravity retaining walls are made or other slope protection methods are followed. Slopes become safe once any of the previously mentioned protective works are done. But during the process of protection works, it is necessary to cut or excavate the slopes and these are at a higher risk of failure. Most of the accidents take place during such excavation and it was reported in Japan that 32 lives were lost due to such slope failure accidents in the year 2003. Fig. 1 shows one of such sites (Bandai-mountain of Fukushima, Japan) where such slope failure accident took place. Slope failure in this site took place when the toe of the slope was excavating in order to construct a retaining wall. In order to prevent the slope failure during such excavation works one should understand the failure mechanism of slope so that a safe and economical method of excavation work could be done.

¹⁾ Research Resident (Rank 'A'), National Institute of Industrial Safety, Kiyose, Tokyo, Japan. (sbtamrakar@hotmail.com)

²⁾ Senior Researcher, National Institute of Industrial Safety, Kiyose, Tokyo, Japan. (toyosawa@anken.go.jp)

³⁾ Researcher, National Institute of Industrial Safety, Kiyose, Tokyo, Japan. (k-ito@anken.go.jp)

⁴⁾ Department chief, National Institute of Industrial Safety, Kiyose, Tokyo, Japan. (horii@anken.go.jp)

⁵⁾ Master Student, Musashi Institute of Technology, Tokyo, Japan. (g0465006@sc.musashi-tech.ac.jp)

In this research, failure mechanism of slopes during the excavation of lower part (toe) of the slope is studied with the consideration of trench excavation at the toe before or after the toe excavation at different soil strength using an in-flight excavator machine which could be used in the centrifugal environment.



Fig. 1 Slope failure due to excavation

EXPERIMENTAL SET UP

In this experiment, soil samples are collected from the above mentioned slope failure accidental site. This soil is classified as SV (Sandy, Volcanic Ash). Grain size distribution is shown in Table 1. Standard compaction test is also performed and its results are shown in Fig. 2. Model ground is prepared in a model box (Fig. 3) with static compaction using bellofragn cylinder. Inner size of the model box is as follows: 45 cm x 15 cm x 27.2 cm. Model ground is prepared by compacting soil into 12 layers; each layer is of 2 cm thick and it is compacted for 5 minutes. Kaoline is spread in between each layer. This facilitates to observe the failure plane and hence failure pattern. In addition, thickness of each layer could also be confirmed.

Table 1: Grain size distribution of Volcanic Sand

Sand (0.075~2mm) %	81.2
Finer particles (<0.075mm) %	18.8
Silt (0.005~0.075mm) %	12.4
Clay (<0.005mm) %	6.4
Max diameter of particle mm	2.0
Uniformity coefficient (D_{60}/D_{10}) U_c	18.2
Classification	SV

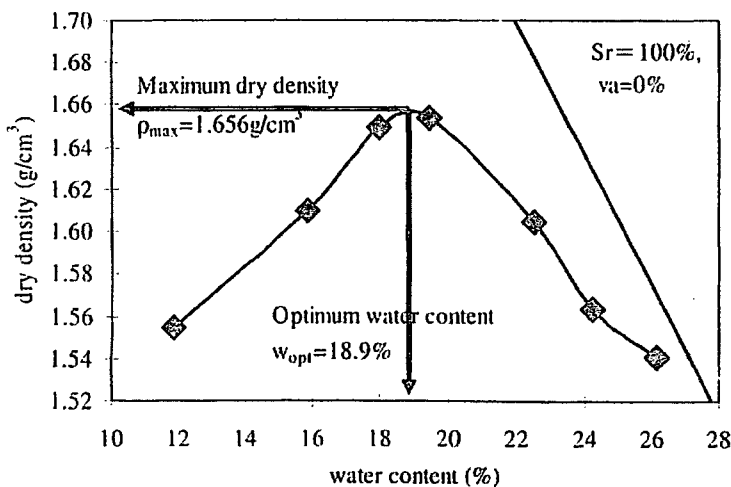


Fig. 2 Compaction curve

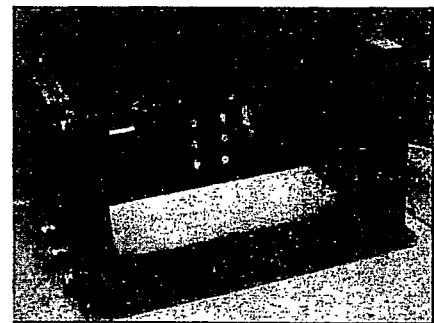


Fig. 3 Model box

Water content of the sample is maintained around 18% which is closer to its optimum moisture content (18.9%). Model ground is prepared under three compaction pressures; 100, 150 and 200 kPa. Once the model ground (45 cm x 15 cm x 24 cm) is taken out from the apparatus box, its front and back panels are removed and the model ground is cut in to the 60° slope angle. Final shape of the model ground is shown in Fig. 4 and 5. The slope angle referred here is according to the safety guideline given out by the Labour Safety and Health Regulation.

Once the model slope is ready, then the side panels; with glass (Fig. 6) and without glass were attached to the model slope ground. In order to reduce the friction between the model ground (soil) and the model box panels, rubber membrane is placed in between. This rubber membrane (Fig. 6) is of same size as that of the model slope ground. Also, a thin film of silicon

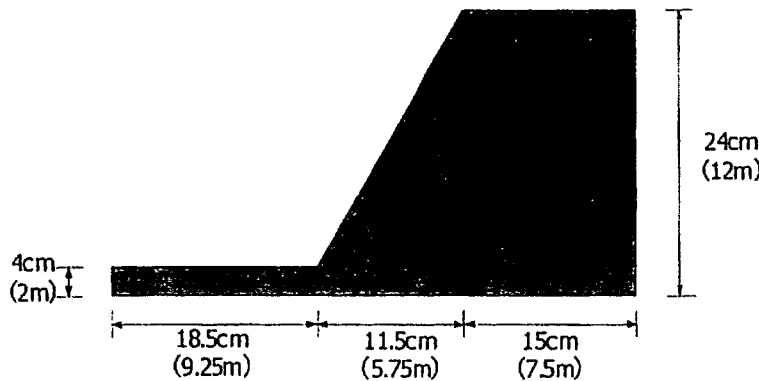


Fig. 4 Final Mod ground (nos. in side the bracket represent the real dimensions when run under 50G)

grease is applied in between the membrane and the panels. More friction could be reduced with it. Finally, whole the model box and model ground are moved down into the platform of the centrifuge. Direct contact type deformation transducers (LVDTs) are placed on the slope and on the top surface of the slope as shown in Fig. 7. Location of each LVDT is marked by x sign. Two LVDTs (S1 and S2) are placed on the slope and another 5 LVDTs (V1, V2, V3, V4 and V5) are put on the top surface. Once the set up is finished, the whole model box is placed on the swinging platform of the centrifuge.

grease is applied in between the membrane and the panels. More friction could be reduced with it. Finally, whole the model box and model ground are moved down into the platform of the centrifuge.

Direct contact type deformation transducers (LVDTs) are placed on the slope and on the top surface of the slope as shown in Fig. 7. Location of each LVDT is marked by x sign. Two LVDTs (S1 and S2)

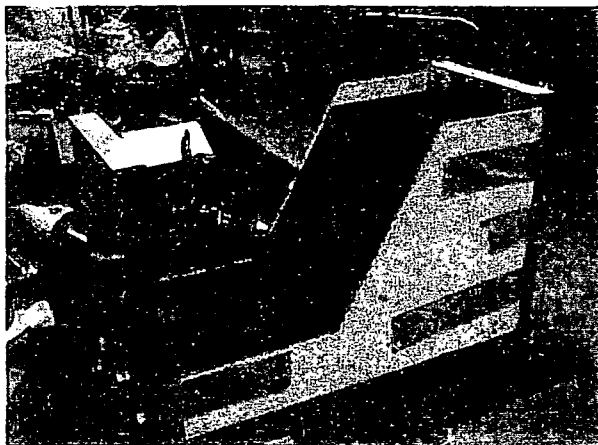


Fig. 5 Model Slope ground

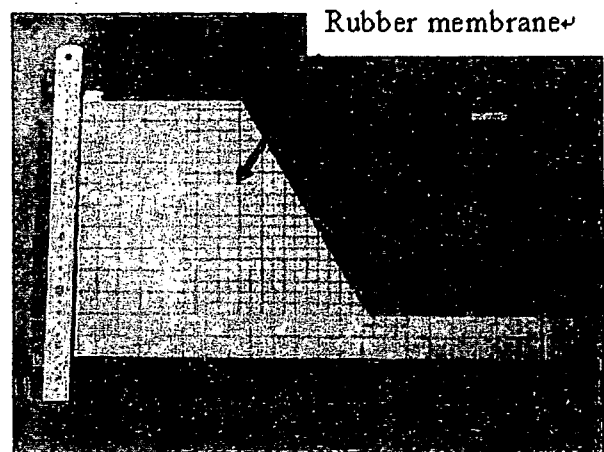


Fig. 6 Rubber membrane on the glass pan

MARK-II CENTRIFUGE

Mark-II centrifuge (Fig. 8) is the new type of effective and multifunctional medium sized centrifuge, which was reconstructed in National Institute of Industrial Safety, Tokyo, Japan. As in other centrifuges, it consists of a main shaft, a drive unit, two arms, two swinging platforms,

a signal and power supply interface and a control box. But unlike in other centrifuges, end portions of its arms are asymmetric. In one end of the arm, solid 'U' shaped structure having a back plate is provided. In this back plate, swinging platform could be fixed as per the requirement by using a pair of hydraulic suspension jacks when the platform is lifted up. This type of system is called "Touch-down system" and it facilitates the simulation of strong earthquake motions in case of dynamic tests (e.g. Shaking table). Other end of the arm is also provided with U-shaped structure without a back plate. This place is used for non-shaking or static tests. Since the back plate is not provide in this side, larger platform, longer arm and a lager working area could be possible. Back plate weight of dynamic side is balanced by hanging counter-weights along the two sides of the static side.

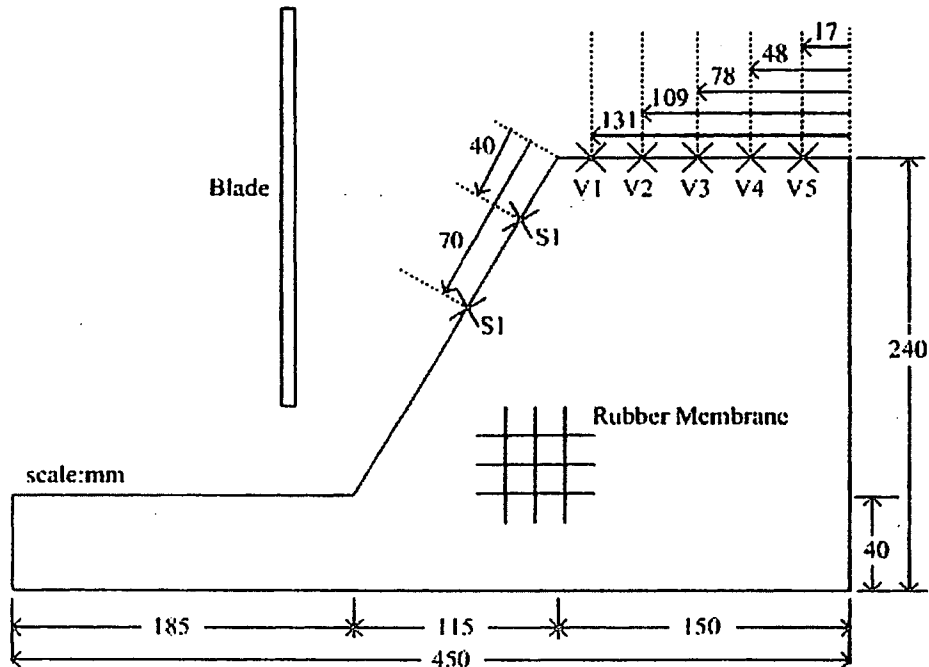


Fig. 7 General layout of the model slope with displacement transducers

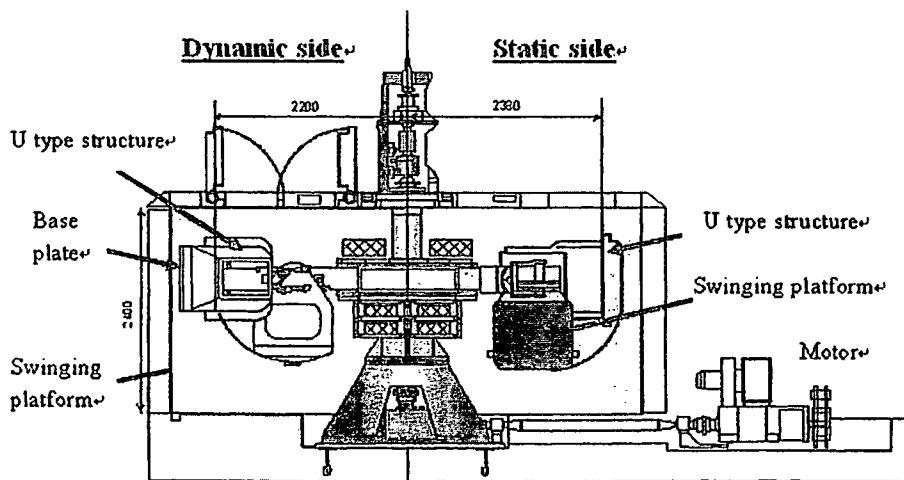


Fig. 8 Mark II centrifuge

In-Flight Excavator

With the change in the stress condition of the ground, its strength and deformation also changes. Therefore, it is necessary to reproduce the actual excavation process in the centrifuge model test also. Various methods of reproducing the process of excavation in the centrifuge model tests were used in the past. For example, cutting up the section, which is to be excavated beforehand from the model ground and then inserting a rubber bag filled up with the liquid at the cut portion and finally, draining out the liquid from the rubber bag during the centrifuge test. But with this method, there was a problem that resistant pressure of passive side can not be reproduced as the excavation section is liquid.

In order to solve this problem Toyosawa et al. (1998) developed an in-flight excavator (Fig. 9) and its specification is given in Table 2. This device is provided with a screw auger which could be used for discharging the excavated soils out side the model box.

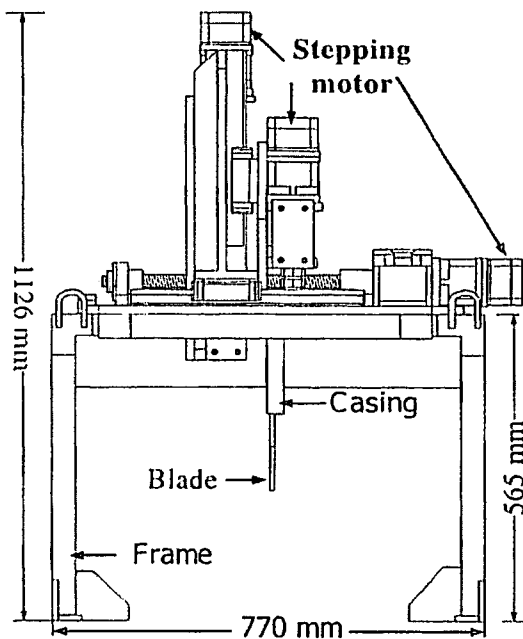


Fig. 9 Fix excavator

The excavator could dig 10 cm x 20 cm or 10 cm x 10 cm section in one dig with 20 cm depth. All the processes of excavation are controlled by 4 stepping motors. This in-flight excavator can be controlled manually or in semi-automatic way from the operating room. Maximum rotation of the auger is 35 rpm and the ascent and descent speed of the auger is 5 mm/sec and drifting speed is 5 mm/sec. In addition, it is possible to replace the auger by blade which could be moved up,

Table 2 Specification of the In-Flight Excavator

Size	Excavator	W770 x D545 x H1126 (mm)
	Controller	W500 x D275 x H425 (mm)
Weight	Total	200 (kg)
	Excavator	139 (kg)
	Stand	61 (kg)
Excavation block	Rotation speed	0~35 (rpm) (0.1 step)
	Motor	370 (kgf.cm) Stepping motor with Harmonic reducer max torque: 36.3 (N.m)
	Speed sensing	Optical sensor
Top-end of excavation block (changeable)	For excavation without sheet pile	W 110 x 100(mm) x 2 lines
	With sheet pile	W 110 x D100(mm) x 2 lines
	With sheet pile and wall	W 110 x D92(mm) x 2 lines
Elevation block	Elevation height	230 (mm)
	Limit sensing	Photo micro sensor
	Speed	0~5 (m/sec) (0.1 step)
	Motor	370 (kgf.cm) Stepping motor with Harmonic reducer max torque: 36.3 (N.m)
Horizontal motion block	Elevation height	260 (mm)
	Limit sensing	Photo micro sensor
	Speed	0~5 (m/sec) (0.1 step)
	Motor	370 (kgf.cm) Stepping motor with Harmonic reducer max torque: 36.3 (N.m)
Control and measurement	Control method	Manual and automatic operation by PC
	Program language	C Language
	Measurement	Speed and displacement of excavation

down, left and right in a horizontal direction. This enables the excavation of the soil ground in a horizontal direction making it possible to shift away the excavated material smoothly from the slope.

EXPERIMENTAL CONDITIONS

Model soil ground are prepared under three compaction pressures; 100kPa, 150kPa and 200kPa. During the centrifuge test, two types of excavation procedures are followed depending upon the trench and toe excavating steps. Types and cases of the experiment are shown in Table 3. In the first type (100 kPa, 150 kPa-Case1 and 200 kPa), excavation was at first started from the toe of the slope. At the end, before the failure, trench excavation is made (except for the model ground 100 kPa) from the excavated portion of the slope itself. In the second type (150 kPa-Case2), trench and slope excavations are started from the beginning and followed up to the end (failure). Two types of excavations followed for the model ground compacted at 150 kPa are shown in Fig. 10. Excavation steps are represented by 1, 2, 3, and so on. All the experiments with the excavation are carried out at 50G.

Table 3 Excavation case and step

	Excavation	First Step
100 kPa	Toe	Toe only
150 kPa-Case1	Toe+Trench	Toe
150 kPa-Case2	Toe+Trench	Trench

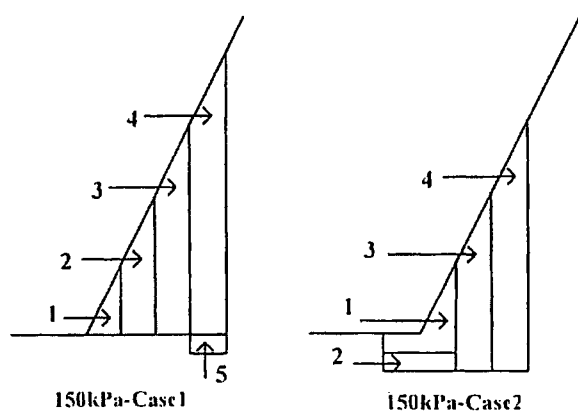


Fig. 10 Excavation Steps

TEST RESULTS AND DISCUSSIONS

The maximum height just before the failure for the all the model tests are shown in Table 4. Comparing the vertical height of the model test just before failure it is observed that there is increase in the vertical height just before failure with the increase in the compaction pressure. Because strength of the model ground increases with the increase in the compaction pressure and this finally increases the vertical height of the slope. But comparing the vertical heights of 150 kPa-Case1 and Case2, the effect of type of

excavation at the toe of the slope could be seen. Vertical height for the Case2 is lower than that for the Case1. This implies that if the excavation of the slope at the toe is made without any trench at first, it can give longer vertical height than that for with the trench excavations from the beginning. This might be the resistive force that would be given by the soil layer at the toe. In 150 kPa-Case1, as the toe of the slope is excavated without any trench at the beginning there is reduction in the failure moment to some extent. Resisting force is given by the soil lying below the toe. In 150 kPa-Case2, slope becomes unstable as there is no soil ground at the trench area to reduce such resistive is present as it has no resistive force the bottom. Table 4 also shows the vertical height if the excavation is done in the real ground.

Table 4 Experimental results

Model No.	At the failure time		
	width	height	Height in reality
100 kPa	1.8 cm	2.8 cm	1.4 m
150 kPa-Case1	3.8 cm	8.0 cm	4.0 m
150 kPa-Case2	2.6 cm	6.0 cm	3.0 m
200 kPa	4.7 cm	9.0 cm	4.5 m

Fig. 11 and 12 show the model ground after failure for 150 kPa-Case1 and 150 kPa-Case2. Solid longer broken line shows the original ground (slope) while the dotted line shows the failure plane. Vertical crack is at the top surface and extended up to some depths. This is followed by the circular failure plane.

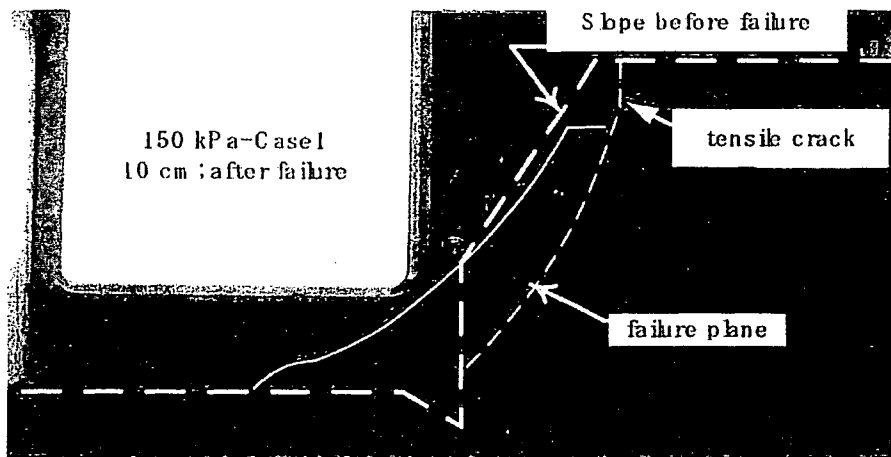


Fig. 11 Model slope after failure for 150 kPa-Case1 (10 cm inward)

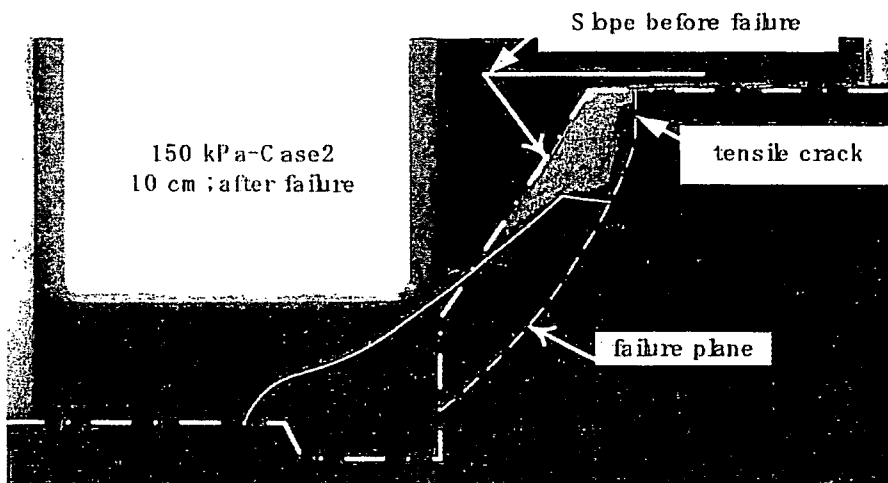


Fig. 12 Model after failure for 150 kPa-Case2 (10 cm inward)

Centrifuge test results for these two cases are shown in Fig. 13 and 14, respectively. In these figures, starting time for each step of excavation time is shown. Comparing the vertical displacements (deformations) on the slope top, it is found that the displacement near the slopes is large and it decreases at the positions farther from the slope. In addition, at each step of excavation, rate of change of deformation values are larger and steeper. In Fig. 15, displacement of the VI (refer to Fig. 7) displacement gauge just before the failure is shown. According to Saito (1969), in the graph of the elapse time and deformation, one could distinguish 2nd degree creep with constant velocity and 3rd degree creep with faster increment in the displacement with time (acceleration) which will proceed to failure. Similar nature of the displacement-time graph is seen in Fig. 15. This suggests that if some kind of displacement is measured during the excavation, possible failure point could be predicted.

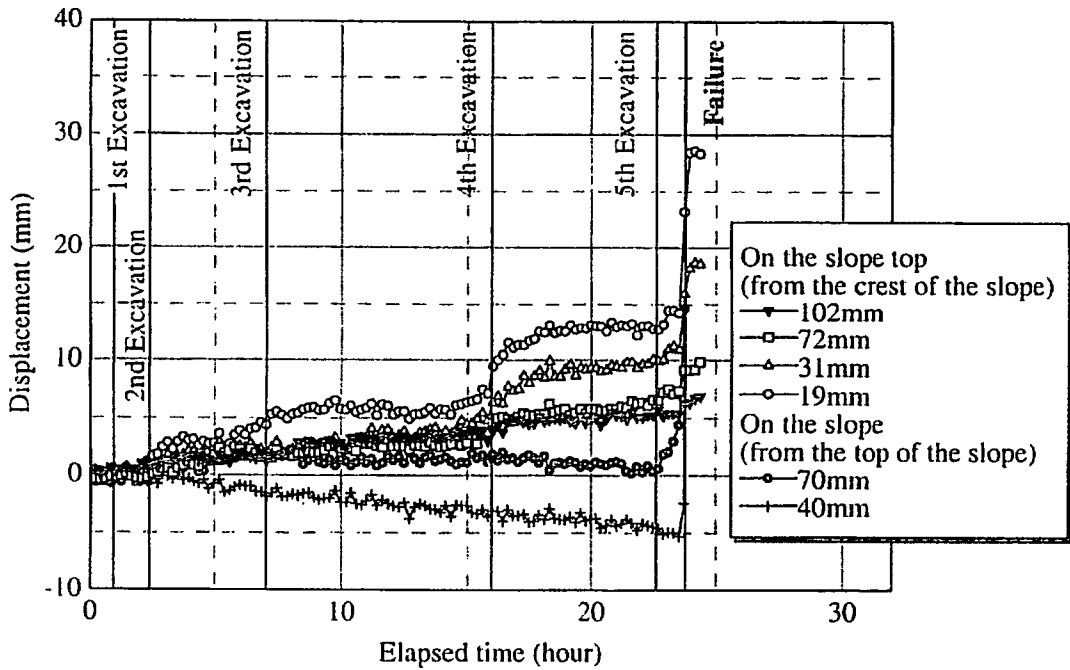


Fig. 13 Displacement vs. elapse time for 150 kPa-Case1 excavation

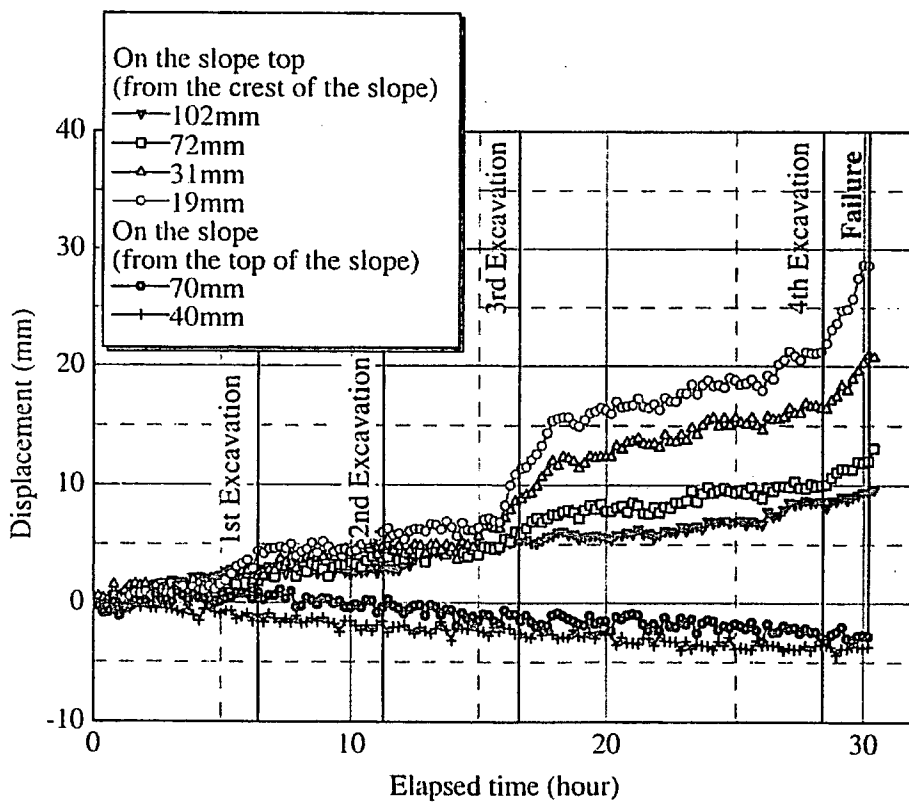


Fig. 14 Displacement vs. elapse time for 150 kPa-Case2 excavation

Fig. 16 shows the displacement of displacement gauge positions from the crest of the slope for 150 kPa-Case1 and 150 kPa-Case2. Displacements are calculated just after each step of excavation after averaging. From the graph, it could be said that with each step of excavation, the crest of slope deformed downward and outward of the slope. But with each step of

excavation, displacements measured on the slope move upward. This implies that with each step of excavation, the volume of the soil on the crest move downward and outward from the slope. Keeping this in mind and looking at Fig. 8 and 11, it could be stated that circular failure had occurred. Vertical crack could also be seen in these photographs although they are smaller in depth.

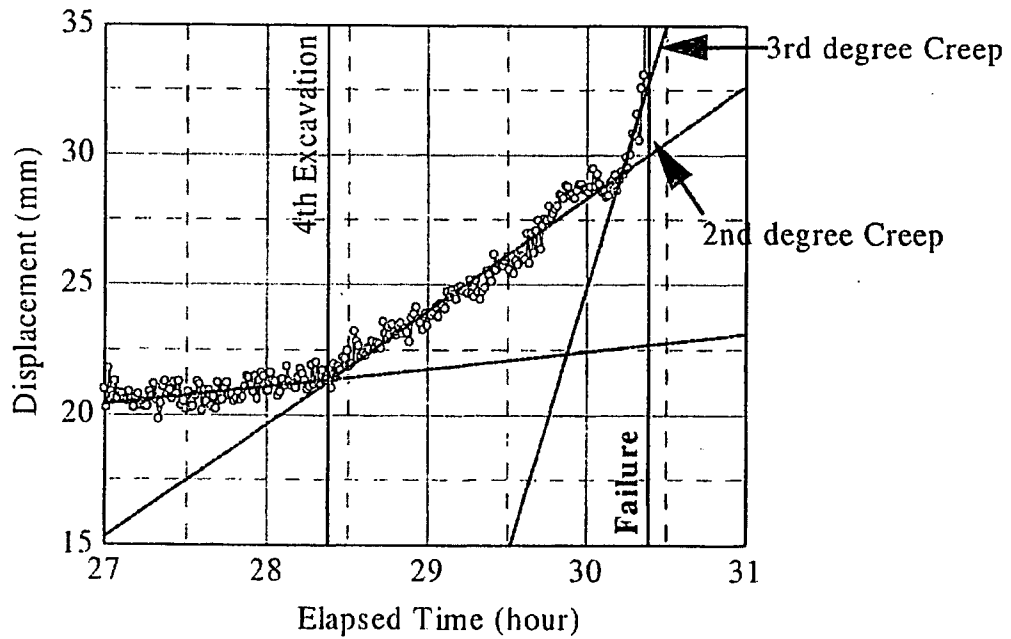


Fig. 15 Displacement vs. elapsed time graph for 150 kPa-Case2

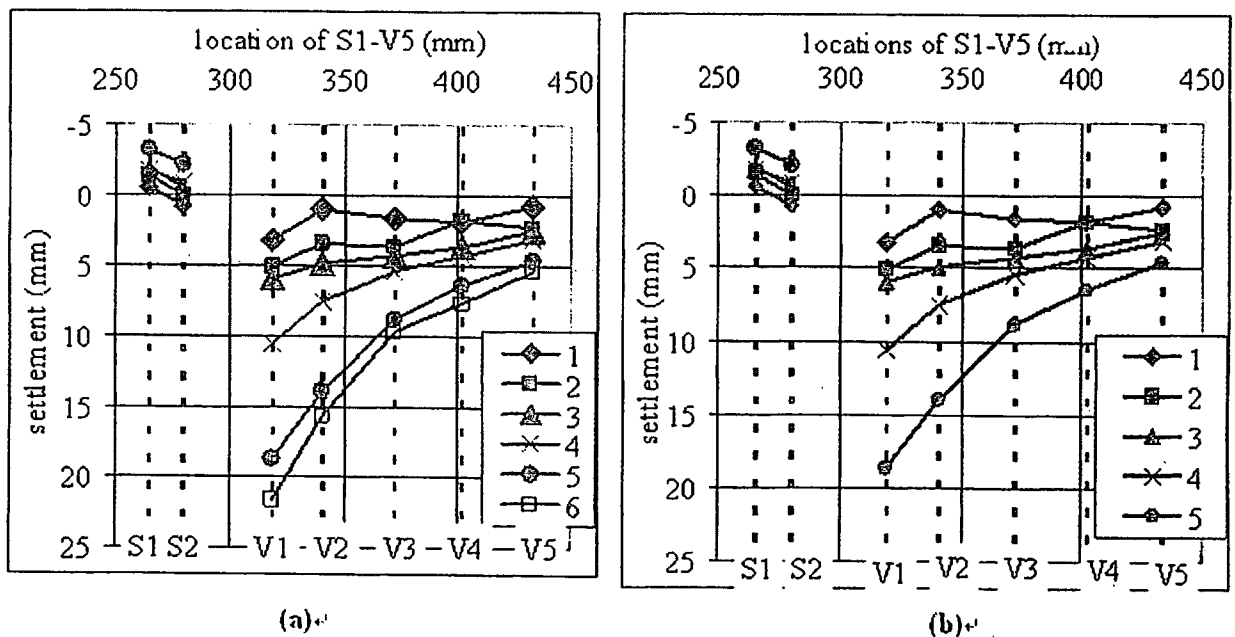


Fig. 16 Displacement and position of displacement gauges (a) 150 kPa-Case 1 and (b) 150 kPa-Case2

CONCLUSIONS

From the centrifuge test results the following conclusions are made:

1. Vertical height of the slope just before failure increased with the increment in the compaction pressure.
2. Vertical height before the failure is larger for the excavation made without trench than the one done with the trench excavation at the start of excavation.
3. Displacement-time graph obtained from the test can be clearly distinguished into the 2nd degree and 3rd degree creep, which might be helpful in predicting possible slope failure time.
4. As seen in most of the slope failure, tensile crack is developed on the top surface which is followed by the circular slope failure.

ACKNOWLEDGEMENT

This research is partially carried out under the Health and Labour Sciences Research Grants of Ministry of Health, Labour and Welfare, Japan. The authors would like to extend their thanks to Mr. Norihiro Yamada of Musashi Institute of Technology, Tokyo, Japan for his help in conducting the test.

REFERENCES

- Saito Michitaka (1969) Research on forecasting the time of occurrence of slope failure. *Soils and Foundations*, 17(2), 29-38.
- Toyosawa, Y., Horii, N., and Tamate, S. (1998) Deformation and failure behaviour of anchored retaining wall induced by excessive excavation in centrifuge model tests. *Research Reports of the National Institute of Industrial Safety (NIIS-RR-97)*, p.35-46.

MEASUREMENT OF SLOPE MOVEMENT DURING THE SLOPE EXCAVATION OF SMALL SIZE FULL SCALE MODEL

Tamrakar S.B.⁽¹⁾, Mitachi, T.⁽²⁾, Toyosawa, Y.⁽³⁾, Itoh, K.⁽⁴⁾ and Airki, T.⁽⁵⁾

ABSTRACT

The main purpose of this research is to develop some kinds of measuring instrument, which could measure the slope movement either directly or indirectly in the real excavating field with which the pattern of failure could be predicted in advance. In this report, slope excavation is carried out with a small size full scale test model made using River Sand. A new instrument, which is a kind of acceleration sensor, called hereby a Tilt-sensor, is used along with laser sensors and linear variable differential transducer (LVDT) to measure the movement of the slopes and top surface of the slope (crest). Changes in the slope angle measured by this new tilt-sensor and the deformations measured by laser sensors and LVDTs on the slope and top surface of the slope (crest) due to the excavation of trench and toe of the slopes showed similar trend. Therefore, applicability of tilt-sensor could be thought of in the field where real excavation is carried out.

KEYWORDS: Slope movement, Tilt-sensor, Slope excavation.

INTRODUCTION

There are many accidents in which workers are injured or dead due to the sudden slope failure in the excavation sites. In almost all of such accidents, stability of the slopes is thought for the final (completed) slopes only and safety analysis is carried out only for the final step. Stability analysis is generally not carried out and thought during the middle stages of excavations. In such situation, even if some unstable sites are found, which may slide (fail) immediately, it might not be possible to repair them instantly. Although complete protection of such slope failure is not possible, it might be possible to prevent the damage due to slope failure to minimum by using fences or cover-ups, which might decrease the speed of the failure or reduce the amount and flow of soil debris. But it is not good to depend upon such protection measures, which have limitations in its protection. It is difficult to prevent the failure or collapse completely and perfectly. But it would be good if one could predict the time of collapse in advance during the excavation which might decrease the damage.

(1) Research Resident (Rank 'A'), National Institute of Industrial Safety, Kiyose, Tokyo, Japan. (sbtamrakar@hotmail.com)

(2) Professor, Hokkaido University, Faculty of Engineering, Hokkaido, Japan. (mitachi@hokudai.ac.jp)

(3) Senior Researcher, National Institute of Industrial Safety, Kiyose, Tokyo, Japan. (toyosawa@anken.go.jp)

(4) Researcher, National Institute of Industrial Safety, Kiyose, Tokyo, Japan. (k-ito@anken.go.jp)

(5) Former Researcher, National Institute of Industrial Safety, Kiyose, Tokyo, Japan. (t-ariki@d-aced.fusione.co.jp)

Measurement of the displacement and deformations of ground surfaces are generally carried out at the construction sites such as embankments and reclamation sites. Doing such measurements, one can know the amount of settlement and the flow direction, which facilitates the construction management to go smoothly and a good maintenance even after the completion of the construction works. In the past and recently, many researches have been presented various methods of measuring the movement of the slope. Japanese Geotechnical Society has given four standard methods for the measurement of the settlement and movement of the slope. Accordingly, in those methods following things are mainly used; 1) settlement plate (JGS 1712-2003)⁽¹⁾, 2) displacement wedges (JGS 1711-2003)⁽²⁾, 3) portable extensometers (JGS 1725-2003)⁽³⁾ and 4) water levelling tube which measures the angle (JGS 1721-2003)⁽⁴⁾. Among these, the first two methods are applicable to construction works such as embankment above the soft ground. The latter two methods are generally used to measure the movement of the land slide. But all of these methods require some fixed points. In addition, they are time consuming and difficult to set up in the actual real field where slope excavation is going on. In the excavating field where the continuous observation is needed to inform the workers about the current status and to make them escape before the quick failure, the above mentioned methods are not proper. Many new methods have been introduced using Optical Fiber Sensors, Non-Prism Total Station, 3-D Laser Scanner, Optical Fiber Extensometer, Fiber Bragg Grating (FBG), Brillouin Optical Time Domain Reflector (B-OTDR) etc. All of these are difficult to set up, handle and maintain the sensitivity. In addition, these new methods costs too much.

In this research, with the purpose of predicting the movement of slope in some kind of shape in advance, measurement of slope movement during the excavation and just before the slope failure was made by using a new tilt-sensor which measures the slope-angle along with laser sensors and LVDTs. Authors have utilized this type of sensor for the first time in out research. Tilt-sensor is in fact a kind of acceleration measuring sensor which is use in the motor vehicles. Here, applicability of this tilt-sensor is checked using a small size full scale test model inside the laboratory so that it could be used in the field. The slopes became unstable by excavating the trenches at the toes of the slope. Excavations were continued until the slopes came to complete failure. Finally, comparison of movements (both deformations and angle) of the slope and top surface of the slope measured by the laser sensors, LVDTs and tilt-sensors was made from the beginning to the end until the slope failed. Similar trend for deformation and change in the slope angles with the time was found.

SMALL SIZE FULL SCALE TEST

Full scale test box

In order to carry to out the small size full scale test in the laboratory, a full scale test box was made. Framework of the test box is constructed from the wooden planks, which are supported externally by the iron plates/beams. The whole framework is divided into two sections; lower (1.35m x 2.7m x 1.3m) and upper (1.35m x 1.2 x 0.88m) which facilitate to make different types of slopes with different conditions. Test box could be assembled either with lower section (Photo 1) only or with the combination of lower and upper sections (Photo 2). If the slope

height is lower or equal to 1.3 m, then the lower section is sufficient to make the test. In the case where the required slope height is larger than 1.3 m, upper section is allowed to attach to the lower section. Since the frontal section of this combined structure is 1.3 m, the test with slope height smaller than equal to 1.3 m is also possible. In this case, load of the material in the backside should be considered as the surcharge. Here, model test slope with lower section only is named as “One-step, Short” (Fig. 1). Model test slopes using the combined structures are divided into two groups. If the model test slope uses only the frontal part, then it is termed as “Two-step, Short” (Fig. 2). Similarly, the model test slope using both the upper and lower sections is termed as “Two-step, Long” (Fig. 3). In this research, these three types of model tests are performed.

EXPERIMENTAL CONDITIONS

Full scale test model

River sand was used as the test material. Here, medium dense test model was tried to obtain. Manually compaction was done in layers by tamping the spreaded sand by foot and small wooden planks. In order to reduce the friction between the inner walls of the test box and sand, inner surfaces were made smoother. Once the compaction was over, wooden planks of the front as well side faces were removed as per requirement and cutting of slopes were done so that the test model of desired slope angle could be obtained. Here, three types of model tests; “One-Step, Short” (Slope-I-3), “Two-Step, Short” (Slope-V-1) and “Two-Step, Long” (Slope-V-2) were done. Water content, density and slope angle for each test are shown in Table 1. As shown in Figs. 1, 2 and 3, 0.3 m thick base was left at the beginning when the model slopes were made so that trench excavation could be made.

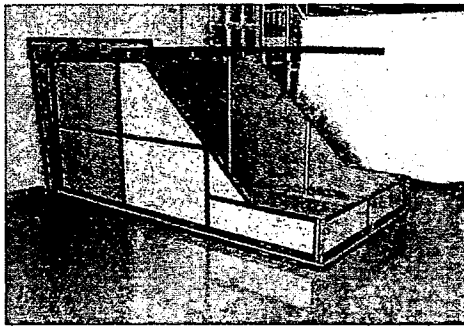


Photo 1 Model box with lower section

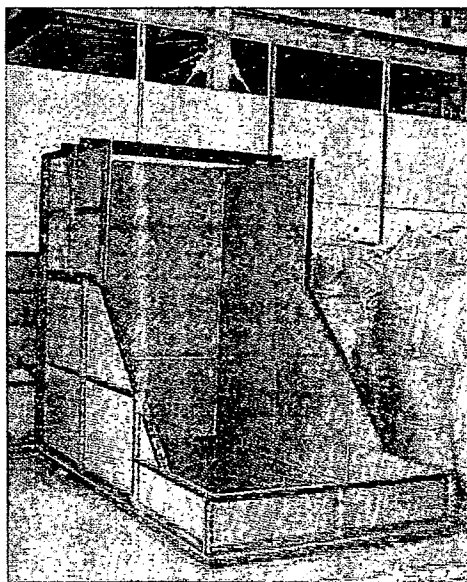


Photo 2 Model box with lower and upper sections attached

As shown in Fig. 4, excavation was done in steps. In Fig. 4, steps are shown by numbers. Number of steps varied with the test as the excavation was tried to make until the slope comes to complete failure. This might be due to the difference in the test conditions including slope angle shown in Table 1. Here, step represents either trench or toe excavations. Trench means the excavation made in front of the toe of the slope and below the ground level. Toe excavation represents the excavation made at the lower section of the slope (toe) and above the ground level. In all the tests, at first, the trench excavation was done. Depth and width of each trench as well as the toe excavation were different. Also, trench after trench and toe after toe

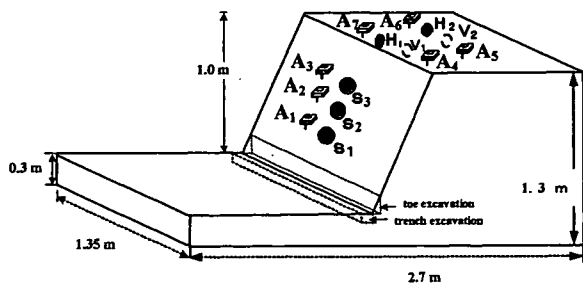


Fig. 1 "One-Step, Short" test model

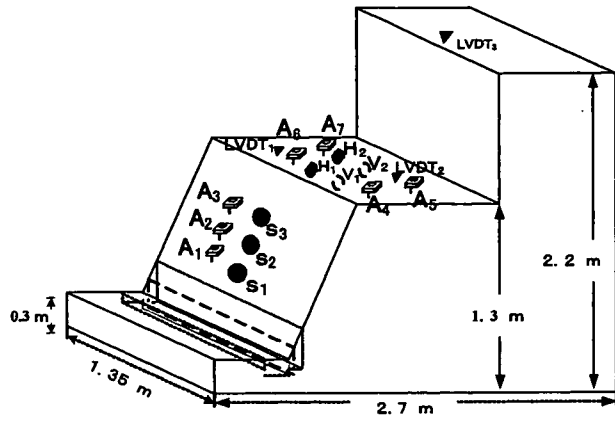


Fig. 2 "Two-Step, Short" test model

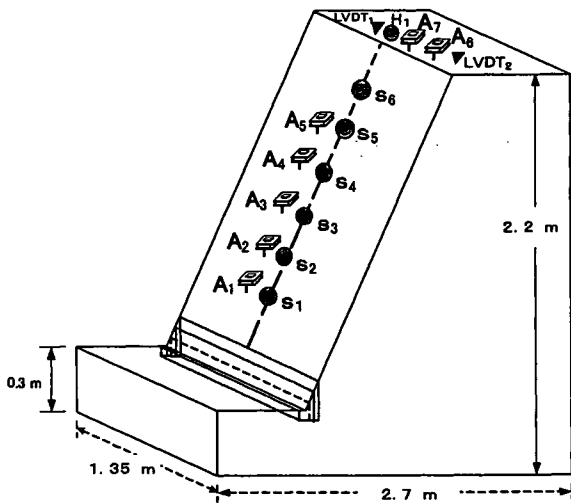


Fig. 3 "Two-Steps, Long" test model

might also be possible. Between each step of excavations, about 5 minutes interval was allowed so that the movement of slopes as well as the top surface of the slope could be observed. In case of Slope-I-3, trench of 15 cm width and 15 cm depth was made at first. Then excavation of toe was done. Slope was failed during the excavation of toe (second step). Quicker failure might be due to low density of the model test (loose compaction). In case of Slope-V-1, total numbers of excavation steps are 21 (Fig. 4(a)). At 12 and 18th steps, trenches were excavated up to the bottom of the test model. Complete failure of this slope took place after 21st excavation step. After removing the failure portion of Slope-V-1, new slope for Slope-V-2 model test was prepared and excavated until slope came to complete failure. In this case, slope came to failure after 7th excavation step. Excavation steps for Slope-V-2 are shown in Fig. 4(b).

Instrumental Set Up

Once the desired slope of the test model was ready, then the set up of measuring instruments was made. Three types of measuring instruments were used. Laser sensor and LVDTs were used to measure the deformation of slope and on the top surface (vertical and horizontal). Tilt-sensor, a new instrument for measuring the movement in terms of angle, was introduced here for the first time.

Laser sensors were attached to the rigid support. Here, H-beams of the test box were used. Target positions for the laser sensors were set up perpendicularly on slope and top surface of the slope. Measurements made on the slope surface with laser sensors gave the slope movement along the failure direction. Slope movements from the laser sensors are represented by S_1, S_2, S_3 , etc. Vertical movement on the top of the slope (crest) are represented by V_1, V_2 , etc., and similarly, horizontal movements are represented by H_1, H_2 , etc. LVDT were used for the vertical

Table 1 Small size full scale test models and conditions

Expt. number	Avg. w	Avg. ρ_d	Slope angle	Type of the slope
	%	g/cm^3	rad	
Slope-I-1	8.35	1.30	50	One-Step, Short
Slope-I-2	8.05	1.30	50	One-Step, Short
Slope-I-3	8.00	1.30	56	One-Step, Short
Slope-V-1	6.6-7.4	1.45-1.50	70	Two-Step, Short
Slope-V-2	6.6-7.4	1.45-1.50	70	Two-Step, Long

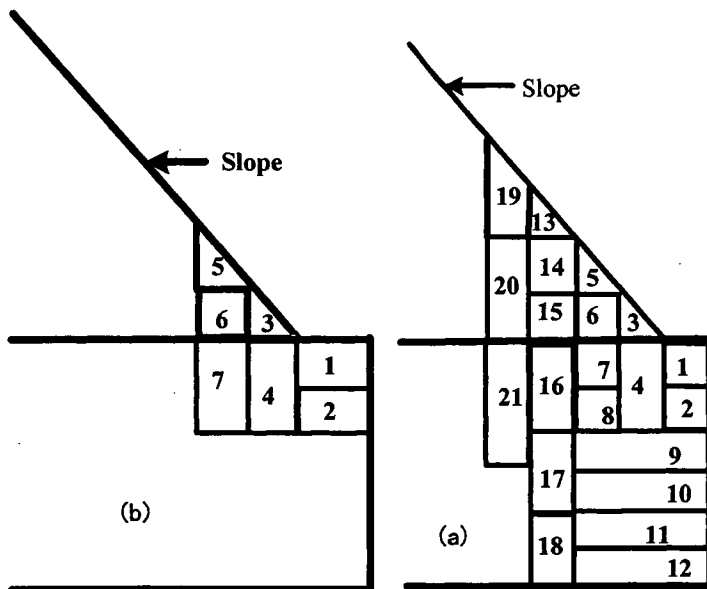


Fig. 4 Steps of excavation (a) for Slope-V-1 and (b) for Slope-V-2

deformations of the top surface of the slope. Tilt-sensors are represented by A_1, A_2, A_3 , etc. Setting up of instruments' locations varied in each test. General layouts of types and positions of instruments were shown in Figs. 1, 2 and 3 for the Slope-I-3, Slope-V-1 and Slope-V-2, respectively. Photo 3 and 4 show the set up for the Slope-I-3 and Slope-V-2 model tests.

Tilt-sensors measure the change in the angle due to the movement of the slope and deformation of the top surface of the slope. In fact, this is an acceleration sensor. It is made in such a way that its output is converted into the angle (degrees). Tilt-sensor used in this research is shown in Photo 5. In Fig. 5(a), its general layout is shown. This

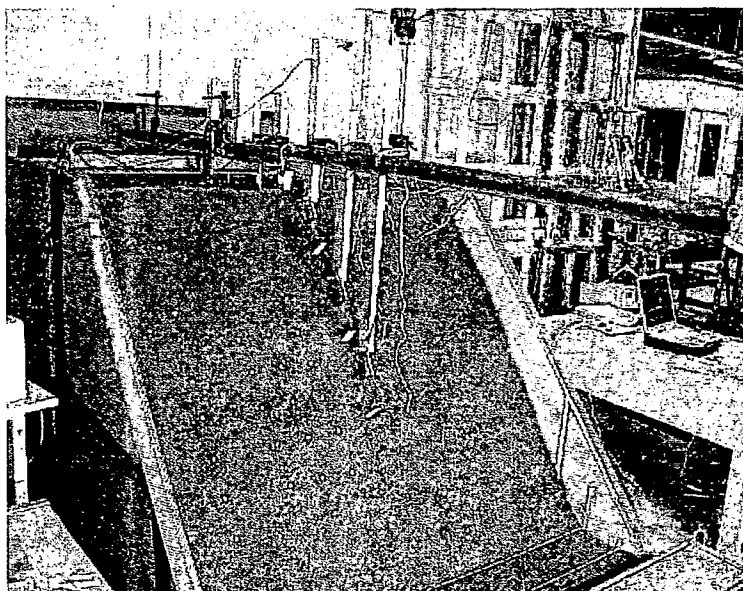


Photo 3 Set up for Slope-I-3 (front view)

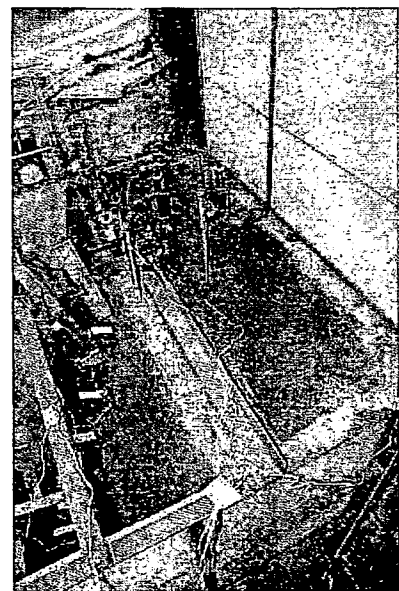


Photo 4 Set up for Slope-V-2 (top view)

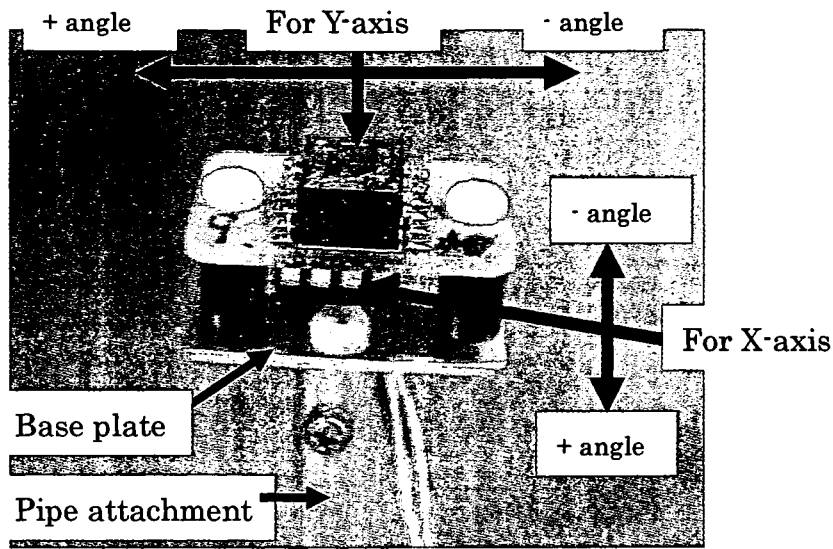


Photo 5 Tilt-sensor used in this research

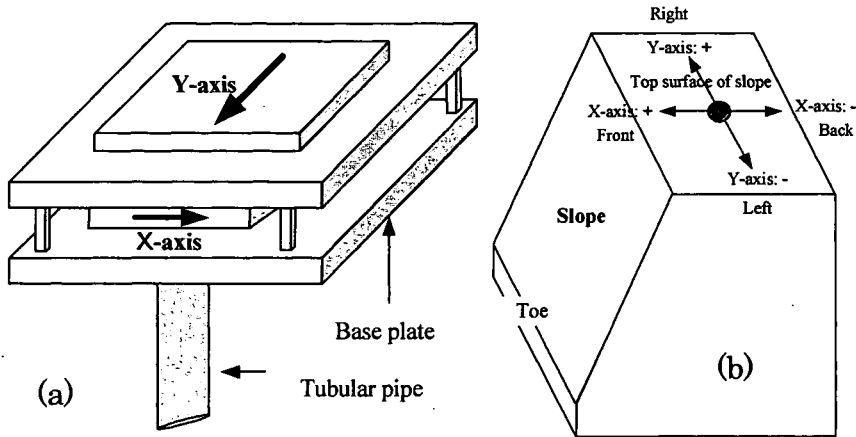


Figure 5 Tilt-sensor (a) General layout and (b) Measuring directions

In Photo 5, tilt-sensor was attached to the base plate which was finally supported by a tubular pipe cut into an angular shape so that it could be easily inserted into the soil without propagating the crack (with less disturbance). Tubular pipe was inserted into the soil in such a way that it could move along with the movement of the slope and deformation of the slope top. To allow the free movement, the longer extension wires were used and they were attached on the sides of the wooden box. Direction of measuring angle from the tilt-sensor is shown in Fig. 5(b). Depth of insertion of tubular pipe into the ground (soil) varied with tests. Length of the pipe could be changed freely. Use of tilt-sensor is first time over here and hence, effect of the length of pipe insertion is a matter of further research. In all the tests here, pipes of tilt-sensor were inserted vertically downward. For Slope-I-3, the depth of insertion on the slope was 25 cm and on the top surface was 10 cm where as for Slope-V-1, it was 5 cm in all the places. But for Slope-V-2, it was 5 cm on the slope and 10 cm on the top surface. Tilt-sensors are represented as A1, A2, A3, and so on (see Figs. 1, 2 and 3). Tilt-sensors were set up near and on the same line of the laser targets. Before the start of measurement, zero set up for all the sensors and LVDTs should be done.

tilt-sensor could measure the angles in X and Y directions as shown in Fig. 5(b). In both the directions, it can measure positive and negative angles. It can measure the angle with in the range of $\pm 20^\circ$ and its sensitivity is 100mV/deg. Thermo-sensor was also attached to this sensor which has the sensitivity of 10 mV/ $^\circ$ C. Tests in this research are carried out inside the laboratory where temperature variation is less. So, temperature is not considered here. But if the tests are to be held in the open field, then the temperature must be taken into consideration using thermo-sensors.

As shown in the Photo